Zeitschrift: IABSE publications = Mémoires AIPC = IVBH Abhandlungen
Band: 35 (1975)

Artikel: A plastic collapse mechanism for compressed plates

Autor: Walker, A.C. / Murray, N.W.

DOI: https://doi.org/10.5169/seals-26940

A Plastic Collapse Mechanism for Compressed Plates

Un mécanisme de rupture plastique pour plaques comprimées

Ein plastischer Bruchmechanismus für gedrückte Platten

A.C. WALKER N.W. MURRAY
Monash University, Department of Civil Engineering, Clayton, Victoria, 3168

1. Introduction

The analysis developed in this paper sets out to explain and predict the manner in which rectangular plates, subject to uniform compression along two opposite edges, behave when they are compressed beyond their ultimate load. The classical elastic theory for the instability of a flat plate [1] and the analysis for the subsequent large deflection behaviour [2] are now well-known. For individual thin plates ($\sigma_y/\sigma_{cr} > 1.5$) the maximum load can be predicted with sufficient accuracy by assuming that when the mid-plane direct stress at some location along an unloaded edge reaches a yield condition the plate will no longer be able to sustain a further increase in loading. The same criterion may be applied to thicker plates, although there is less justification for it, and a semi-empirical design curve has been formulated [3, 4] in which the effects of initial imperfections have been included by using a generalised imperfection parameter.

But, of course, plates in engineering practice are not used in isolation; they form elements in thin-walled structures. If these structures are sufficiently redundant in topology, the failure of a single plate need not mean that the structures as a whole will fail. It is necessary in such a situation, however, to know the load-deformation characteristics of the buckled plates in order that the stiffness and remaining strength of the structure can be determined. Furthermore, a study of the load deflection characteristics during and after buckling not only indicates how suddenly a structure will fail (i.e. how "brittle" or "tough" it is) but also how sensitive it is to initial imperfections. A few analytical attempts to obtain the post-buckling characteristics of plates have been made. GRAVES-SMITH [5] and others at Cambridge used numerical methods to obtain an elasto-plastic solution. They obtained theoretical load-deflection curves for a few plates but the method employed required large amounts of computer time and it appears that for this reason more general studies have not been made. More recently SHERBOURNE *et al.* [6, 7] have used a plastic mechanism method to study the post-buckling behaviour of flat and corrugated plates. Although good agreement between theory and experimental results was obtained in some cases this was not true in others for which the agreement was poor. Sherbourne's analysis assumed a particular shape of mechanism and the plastic unloading line was obtained by allowing the geometric proportions of the shape to vary and determining, by means of a computer, the minimum load corresponding to a specified deflection amplitude.

MURRAY [8, 9] has tested thirteen plates stiffened by bulb flats; these plates were observed to fail either by lateral buckling of the stiffener or by a concertina-like buckling of the plate-deck. It is only the latter case which is considered here. To obtain a theoretical estimate of the plastic collapse behaviour, the geometry of the plastic mechanism (as indicated by laboratory observations (see Fig. 1a)) was assumed and a numerical minimisation technique was employed to fix the size of the mechanism. It was found necessary to use a small – and a large – deflection theory in order to explain the behaviour of these plates. Unfortunately, it was not possible in the experimentation to obtain the plastic collapse line because the apparatus could not follow the unloading which occurred. Thus the theory could not be thoroughly checked against experiment. The theory developed by MURRAY does not explain one observed phenomenon in his study of the behaviour of stiffened plates. He observed in the laboratory that for stiffener buckling sudden collapse occurred as predicted by theory. However, for the concertina-like plate buckling cases failure was somewhat more gradual whereas his theory predicted that the suddenness of collapse would be similar to that for the stiffener buckling cases. In other words, the experimental results crossed the theoretical collapse line (Fig. 1b) and penetrated deeply into a region where failure should have occurred already.

In this paper a similar approach is taken, rigid-plastic analysis is used and results are derived that are in good agreement with experiment. But since this analysis, like the others referred to earlier, assumes a mode of plastic deformation, it is useful to consider the mechanics by which such a plastic mechanism may be formed. To obviate the problems involved in solving the non-linear elasto-plastic plate formulation the phenomena are discussed with reference to simple conceptual models.

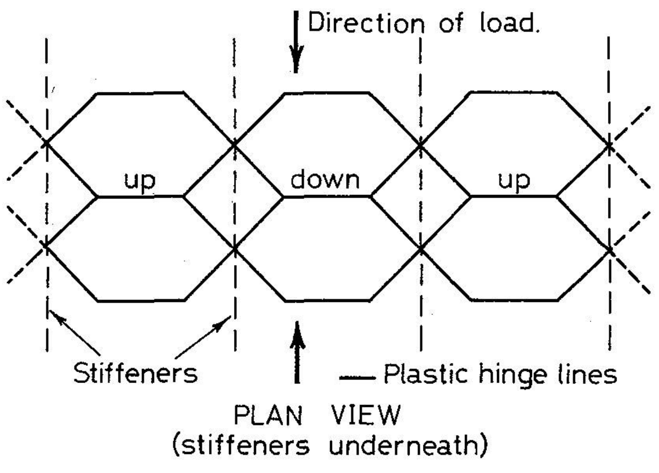

Fig. 1a

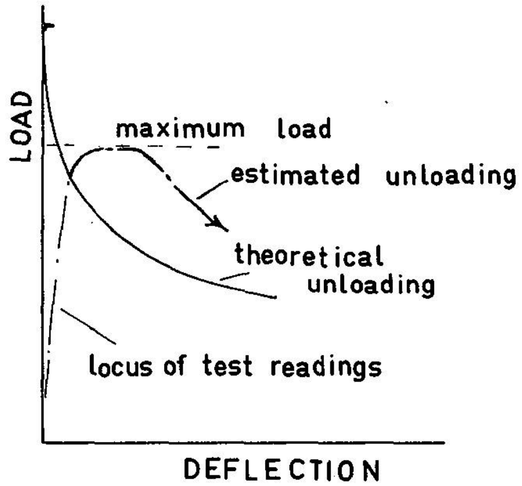

Fig. 1b

2. Concept of Plastic Mechanism

When a structure is wholly elastic the analysis can be performed using the well-established method involving the requirements of compatibility and equilibrium or the equivalent condition of energy extremum. But when the material begins to yield in some region due to the state of stress there, the analytical problems increase by an order of magnitude. Recently, large computers in conjunction with discrete numerical methods, such as finite elements or finite differences, have been used to follow the load-deformation characteristics of simple structural elements as the plasticity spreads due to increased loading. However, even with such machines it is not a simple task and is often costly in machine time. It is therefore not a viable approach for initial design calculations – at least not with today's computers.

An alternative approach has been to assume a state in which the plasticity has spread to such an extent that all the deformations occur in that region and we neglect the deformations that occur in the remaining elastic portion. The behaviour of the plastic portion is itself simplified, without distorting the physics of the region, so that the mathematics become elementary. The type of conceptual model used here is shown in Fig. 2a for elastic behaviour and Fig. 2b for plastic behaviour.

In this, the rotational spring stiffness c models the elastic flexural rigidity of a strut and the curves (i), (ii) and (iii) in Fig. 2c indicate the elastic load-deflection relationship for various values of initial imperfection w_0. Now turning to plastic behaviour we take the particular example of a strut with rectangular cross-section, breadth b and depth d, that is subjected to a moment M_p' and a longitudinal force P; if the material everywhere on the cross-section is assumed to be stressed to its yield stress, the maximum moment it can carry is [10]

$$M_p' = M_p\,[1 - (\frac{P}{P_y})^2], \tag{1}$$

where M_p is the plastic moment $\frac{bd^2}{4}\,\sigma_y$. Putting an equivalent hinge in the middle,

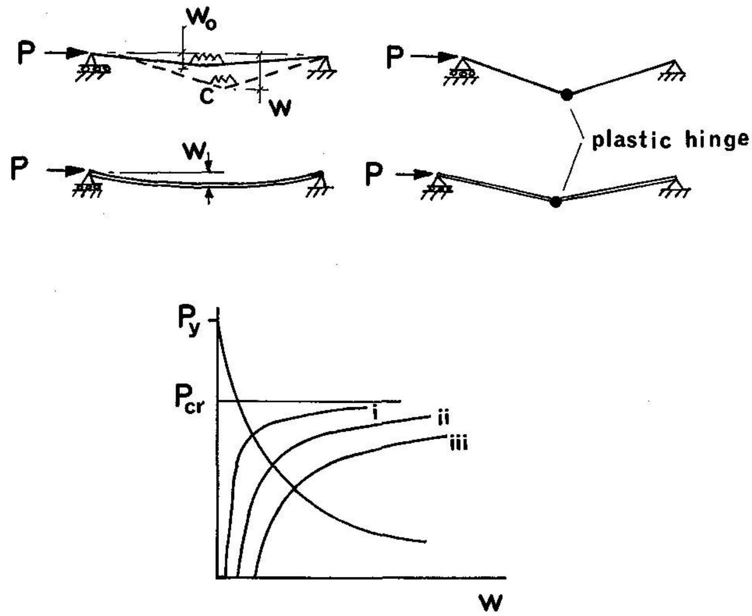

Fig. 2

Fig. 2b, we determine the curve (iv) in Fig. 2c. This method assumes that there is a sudden transition from elastic to plastic mode at the intersection of the curves. Of course in reality there is a gradual spread of plasticity across the section, but because most of the energy in the column in both the elastic and plastic modes is bending strain energy this approach has in the past been a sufficiently accurate and useful aid in describing the behaviour of struts and frameworks [10].

In this paper we are interested primarily in long rectangular plates and it is observed during tests that these will deform into regular wave-like patterns of the type shown in Fig. 3a. Measurements of a typical elastic plate supported at its edges give a load-deflection relationship of the shape indicated in Fig. 3b. If the plate is sufficiently thin it will support axial loads in excess of the critical load

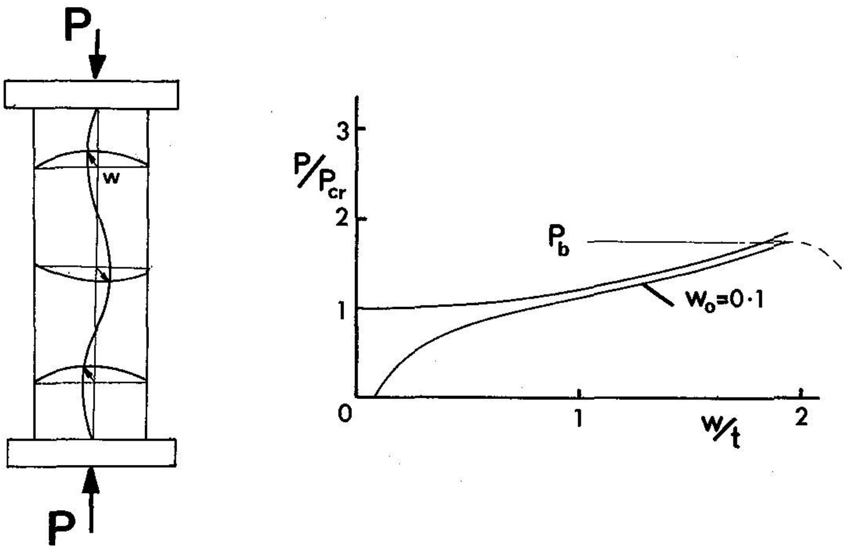

Fig. 3

corresponding to the perfectly flat condition. It is well-known that this increase is due to the restraining effect of the membrane action and that the longitudinal direct stresses become greater at the edges during buckling. As stated earlier, the unloading characteristics of an axially loaded thin plate are difficult to obtain experimentally because collapse occurs very rapidly once a mechanism starts to form. Elastic energy stored as membrane and bending stresses is released during this process and drives the mechanism until its deformations are large. Fig. 4a shows the deformed shape of the mechanism observed for medium-thick steel plates ($\sigma_y/\sigma_{cr} < 1.5$) and Fig. 4b typifies the corresponding shape for thin plates (although the shape shown in Fig. 4a has also been observed).

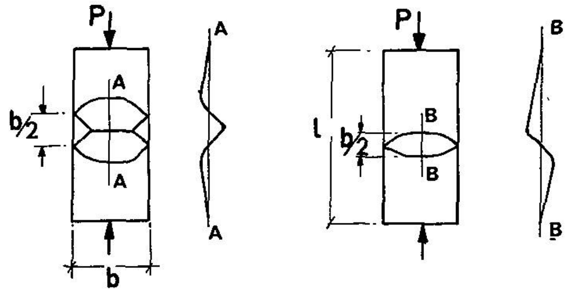

Fig. 4

In the next two parts of this section the simple lumped parameter model introduced in Fig. 2 is extended for the purpose of explaining the physics of elastic and post-elastic plate buckling. This study facilitates the understanding of the phenomena referred to above and, finally, indicates a suitable form of plastic mechanism to be used in the analysis in Section 3. The form of this mechanism is different from that used by MURRAY [9]. Their relationship is discussed in Section 5.

2.1 Square Plate

A simple lumped-parameter model of a square plate that incorporates the stiffening effect of the mid-plane membrane forces is shown in Fig. 5. The longitudinal strip AB is modelled (Fig. 5b) by two longitudinal rigid links and a rotational spring which has a lumped flexural stiffness $c/2$. The lateral strip CD is modelled by two lateral extensional springs of stiffness k and a rotational spring

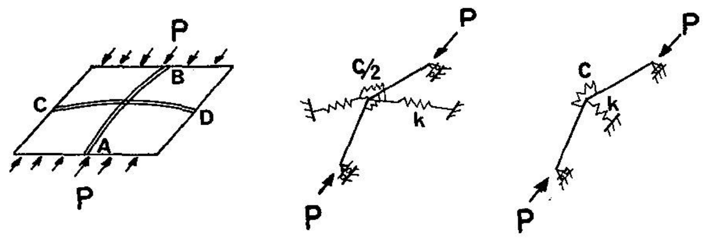

Fig. 5

of stiffness $c/2$. As this model deflects upwards by an amount w the lateral springs each extend, to a first order approximation, by an amount $\frac{w^2}{l}$. Thus the two lateral springs can be replaced by a non-linear transverse spring (Fig. 5c) which carries a load equal to $\frac{4kw^3}{l^2}$. The equilibrium equation for small deflections of this model with no initial imperfections is

$$(4-p)w = k^*w^3, \text{ where } p = \tfrac{Pl}{c},\ k^* \equiv \tfrac{k}{c} \tag{2}$$

and its load-deflection characteristics are shown in Fig. 6. The other graphs in this figure are load-deflection curves when there are initial imperfections. Thus this lumped parameter mechanism models the behaviour of a square plate in the elastic range.

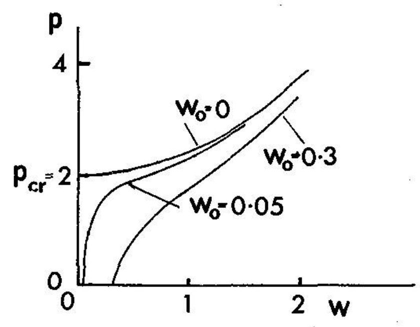

Fig. 6

Up to the initiation of yielding both the extensional and rotational springs maintain their stiffness values, but afterwards the moment at the centre pin may be considered to reach a maximum value of M_p' which is a function of the axial load (see eqn. (1)). The rotational spring must then be replaced by one with zero stiffness because at a full plastic hinge $\frac{dM}{d\theta} = 0$. During the development of the plastic mechanism and as yielding penetrates deeper into the plate the stiffness of the transverse springs (Fig. 5b) is reduced. Eventually when the deflections are large the mechanism yields across the full section and k is then zero. If we assume a value of k that is small relative to its initial value and constant throughout the deformation, the curve *II* (Fig. 7b) is obtained for the mechanism shown in Fig. 7a.

Suppose the model were to be tested in a laboratory. As the load was applied we would expect the experimental points to follow curve *I* until the onset of yielding. Eventually, when the deflections are large the experimental points should become asymptotic to curve *II*. But we should not expect that the points would transfer from curve *I* to curve *II* at point *A*. This is what happens in the case of a simple strut in which nearly all of the energy is flexural, but is cannot happen in the case of the plate model because the stiffness k of the lateral spring (which represents the membrane stiffness) still has its elastic value at point *A*. Thus the rotational spring is restrained from developing its full plastic moment until point *B*. The experimental points will therefore proceed beyond point *A* to near *B* and then droop down asymptotically along curve *III* towards curve *II* but from

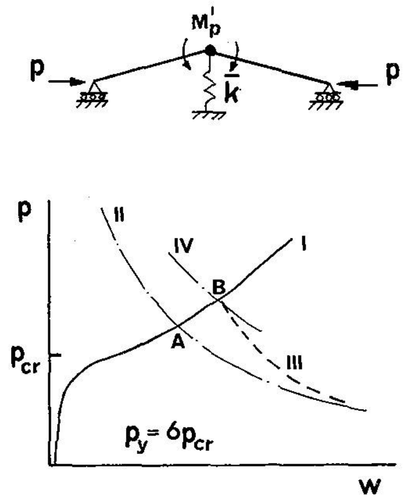

Fig. 7

above. During this stage the value of k is decreasing towards zero. Point B and the actual failure load may or may not be well above A depending on the values of the parameters defining the plate geometry. We can surmise that if the intersection of Curves I and II (Fig. 7b) is used as an estimate of the failure load it will probably, but not necessarily, be conservative.

The position of B (Fig. 7b) for the model shown in Fig. 7a can be found by considering its equilibrium in the same way for the model shown in Fig. 5c. Moments about the left hand end give

$$Pw - M_p' - \frac{kw^3}{l} = 0$$

By using eqn. (1) and after re-arranging we obtain

$$P = \frac{-w + \sqrt{w^2 + \frac{4M_p}{P_y^2}\left[\frac{kw^3}{l} + M_p\right]}}{2(M_p/P_y)^2} \tag{3}$$

This equation is plotted as Curve IV in Fig. 7b and its intersection with curve I defines the point B. As the mechanism develops the value of k decreases (as stated above) and when k becomes zero eqn. (3) gives curve II.

2.2 Rectangular Plate

The model of the previous section can be extended to enable us to study the mechanics of a rectangular plate.

Figure 3a shows a plate with an aspect ratio 3:1 and Fig. 8 its model. We can compute the model's elastic behaviour with a wide variety of initial imperfections. The spacing of the springs and hinges is equal to the half width of the plate and the equilibrium condition is:

Section 1-2: $(6-p)\,w_1 + (-8+p)\,w_2 + 2w_3 = -k^*\,(w_1{}^2 - w_{01}{}^2)\,w_1 + 6w_{01} - 8w_{02} + 2w_{03}$

Section 2-3: $(-8+p)\,w_1+(14-p)\,w_2+(-8+p)\,w_3=2k^*\,(w_2{}^2-w_{02}{}^2)\,w_2+8w_{01}+14w_{02}-8w_{03}$
Section 3-end: $2w_1+(-8+p)\,w_2+(10-2p)\,w_3=-2k^*\,(w_3{}^2-w_{03}{}^2)\,w_3+2w_{01}-8w_{02}+10w_{03}$
where w_{01} is the initial value of w_1, etc., $p\equiv\frac{Pb}{c}$ and $k^*\equiv\frac{k}{c}$ (4)

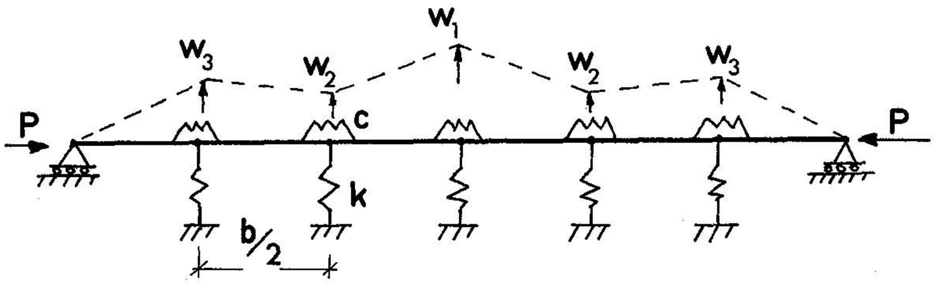

$$(3-p)\ w_1 + (-4+p)\ w_2 + w_3 = -\ k^*(w_1{}^2 - w_{01}{}^2)\ w_1 + 3w_{01} - 4w_{02} + w_{03}$$

$$(-4+p)\ w_1 + (7-p)\ w_2 + (-4+p)w_3 = -2k^*(w_2{}^2 - w_{02}{}^2)\ w_2 + 4w_{01} + 7w_{02} - 4w_{03}$$

$$w_1 + (-4+p)\ w_2 + (5-2p)\ w_3 = -\ 2k^*(w_3{}^2 - w_{03}{}^2)\ w_3 + w_{01} - 4w_{02} + 5w_{03}$$

where w_{01} is the initial value of w_1, $p \equiv \frac{Pb}{c}$, $k^* \equiv \frac{k}{c}$

Fig. 8

In Fig. 9a the initial imperfections indicated cause the model to deform in a uniform waveform. But such regularity in the initial imperfections would be unusual in practice and Fig. 9b indicates the gradual change of waveform as the load is applied to a model with irregular deformations.

For this latter model, the onset of plasticity will occur at the central hinge and, as shown in Fig. 10a for a moderately thick plate ($\sigma_y/\sigma_{cr}\simeq 2$), there is unloading accompanied by reduction of the deflection in the elastic portion until the plastic condition is reached at the adjacent hinges after which a completely local mechanism forms. For a much thinner plate ($\sigma_y/\sigma_{cr}\simeq 6$) the hinges form at both positions almost simultaneously as shown in Fig. 10b.

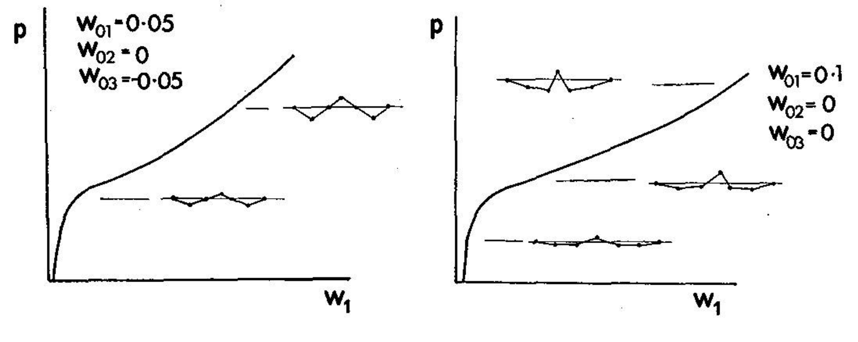

Fig. 9

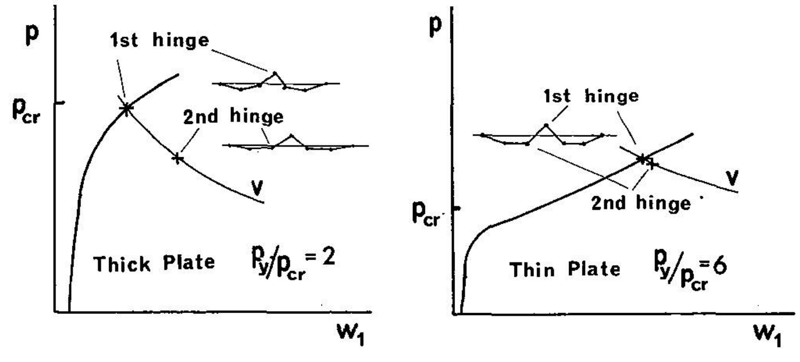

Fig. 10

It is now possible to infer the probable causes for the deformed shapes in Fig. 4. Taking the thinner plate first; as the load is increased, the out-of-plane deformations will grow and their shape will largely be determined by initial geometry. In our model there was symmetry about the central hinge but of course this will probably not occur in the analogous imperfection in a practical plate. When the maximum load is reached, that is after the edge stresses have attained a yield condition, the plate begins to unload. The deflections at the position of yielding increase rapidly and, as indicated by the model, the remaining elastic portion becomes flatter. The plastic moment will be reached at the positions of maximum deflection and a mechanism will start to form. This will have a curved form in plan because the out-of-plane deflections vary across the plate from a maximum at the centre to zero at the edge. This variation is approximately sinusoidal in form so the curve of the yield line is the intersection of an inclined flat plane with a sinusoidal cylinder. Because the plastic hinges form over such a small range of deflection it is easy for one of the outer hinges to form completely before the formation of the other outer hinge is at all started. When this happens it is sufficient that only one side of the mechanism forms for deflection to proceed and the other side flattens out. Because of the asymmetry of the deflections in practice this will occur in most cases.

In the thicker plate there is usually a symmetrical buckled plastic shape and this is in fact the amalgamation of two mechanisms as shown in the thin plate. The reason is that the asymmetry of deflected shape is not so well developed and the separation of the deflections at which the first and second hinges form means that the two outer hinges are forced to form almost simultaneously.

It is interesting to compare this model behaviour to that observed in the laboratory during tests on long rectangular plates ($40 \lesssim b/t \lesssim 60$). As the axial load is increased initial imperfections grow in magnitude and gradually form a regular pattern of elastic waves whose wavelength is approximately equal to their width. At this stage the longitudinal stresses are greater at the edges (where the plate is straight) than at the centreline. Finally the plate yields at the edges triggering the development of a plastic mechanism which initially, for a very uniform elastic deflection pattern, spreads over a large portion of the plate (Fig. 11). But of course some region has a slightly greater deflection and it is noticed that this now begins to deflect at a much faster rate and the other regions begin to flatten out. The result is the local plastic deformed shape indicated in Fig. 4a.

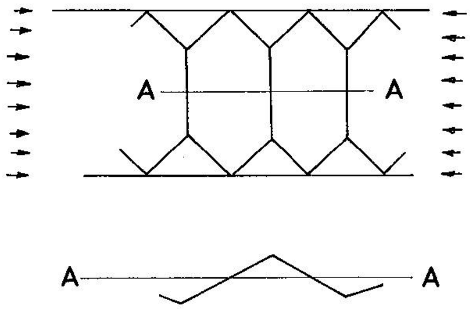

Fig. 11

The model analysis in this section has indicated that the buckled shape of a plate is governed not only by plasticity in the material but also by the initial deformations and the rate of growth of the elastic buckles in that part of the plate that is adjacent to the plastic zone. This, of course, is a very complex problem to analyse mathematically and it is useful to consider approximate, but much simpler, approaches in an attempt to afford some insight to the plate plastic unloading characteristics. One approach would be to assume that the initial deformations were so regular that the buckling mechanism formed simultaneously everywhere in the plate as in Fig. 11. The link and spring analogue of this mechanism is shown in Fig. 9a with the resulting plastic unloading line shown as curve *II* in Fig. 12. This is similar to the model in Section 2.1, it underestimates the collapse load and lies below the actual unloading curve *V*.

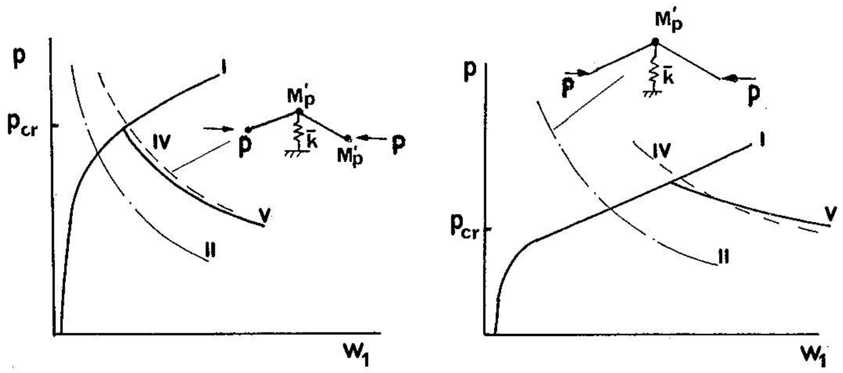

Fig. 12

An alternative approach is to assume that the elastic deflections are zero and that the deformations occur only as a plastic mechanism. A study of Figs 9, 1a and 11 suggest that the mechanism as shown in Fig. 13 will be the one which the plate eventually tries to develop because the hexagonal plates (Figs. 1 and 11) are pivotted along their long diagonal. The length of the link (Fig. 13) is an estimated value.

This model can be analysed simply to give the equilibrium equation:

$$Pw = 2M_p\left[1 - \left(\frac{P}{P_y}\right)^2\right] + \bar{k}w^3 \tag{5}$$

where $\bar{k} = \frac{bk}{2l^2}$ and the corresponding unloading line is shown as curves *VI* in Fig. 12.

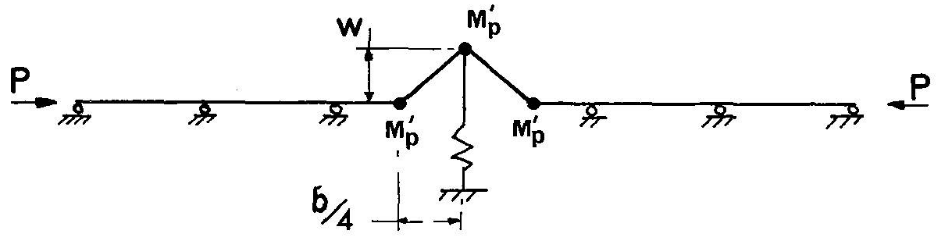

$$Pw = 2M_p\,[1 - (\frac{P}{P_y})^2] - 2\bar{k}\,w^3$$

Fig. 13

In this mechanism we are eliminating the contribution of the elastic portion of the plate but at the same time increasing the amount of plastic energy dissipated by increasing the rotation of the outer plastic hinges. Although this mechanism is not that which corresponds to the exact solution of the problem it serves the purpose of simplifying the analysis and provides a good approximation of the maximum load and the unloading line. In the next section we make a similar simplification for an axially loaded plate and henceforth in this paper we consider only the symmetric buckle pattern.

3. Continuum Analysis

As we have seen the actual buckled shape of a compressed plate is affected by the elasticity of the deflected regions adjacent to the region of plasticity. But the model analysis in the previous section suggests that a modified mechanism in which this elastic energy is eliminated may predict the plate buckling behaviour with adequate accuracy. This modified mechanism is shown in Fig. 14 and in the first instance it is analysed using bending action only. In Section 3.2 membrane deformation is considered.

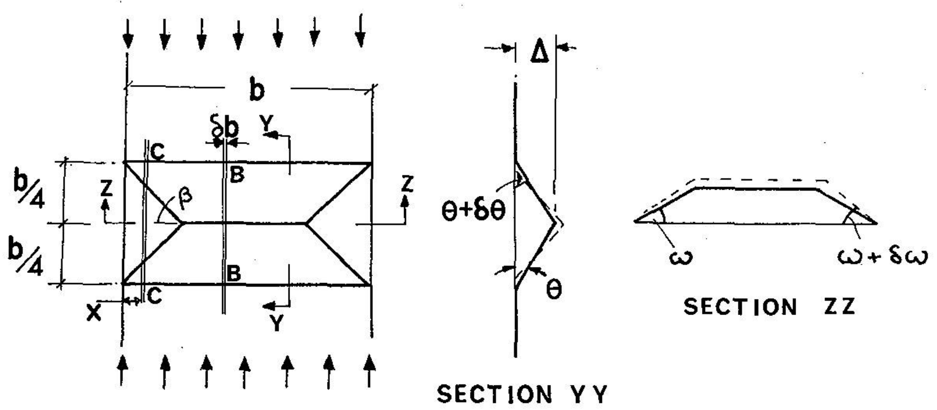

Fig. 14

3.1 Plastic Bending

The theory developed by MURRAY [8] is used here. The plate is considered as being composed of longitudinal strips. There are two typical regions; one containing strips typified by *BB* and another region comprising strips like *CC*. For strip *BB* of width δb (see Fig. 14a and Fig. 15a) the equilibrium equation is

$$P\Delta = 2M_p' \tag{6}$$

that is

$$P = \sigma_y\, t\, \delta b\, [\sqrt{(\Delta/t)^2 + 1} - \tfrac{\Delta}{t}] \tag{7}$$

The width of the region is b $(1 - \tfrac{1}{2} \cot \beta)$ so that the load P_1 that this portion of the plate can support is

$$P_1 = \sigma_y t b(1 - \tfrac{1}{2} \cot \beta)\left[\sqrt{\left(\frac{\Delta}{t}\right)^2 + 1} - \frac{\Delta}{t}\right] \tag{8}$$

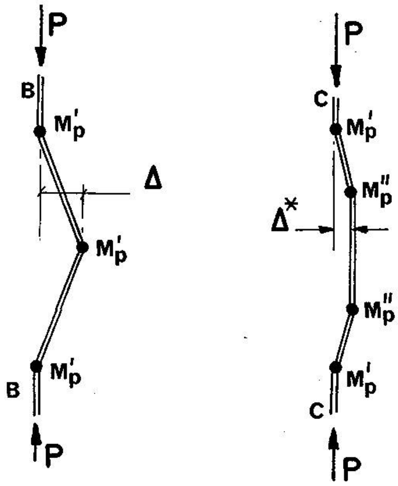

Fig. 15

For strip *CC*, the geometry is shown in Fig. 15b; the inner hinge is inclined in plan at an angle β and MURRAY [11] has shown that for such a situation the effective plastic moment M_p'' is

$$M_p'' = M_p' \sec^2 \beta = M_p \left[1 - \left(\frac{P}{P_y}\right)^2\right] \sec^2 \beta \tag{9}$$

The equilibrium equation for this strip is

$$M_p' (1 + \sec^2 \beta) = P\Delta^* \tag{10}$$

where $\Delta^* \equiv \Delta \dfrac{x}{\frac{b}{4} \cot \beta}$

and x is the distance of the strip from the plate edge. The load P_2 carried by these outer regions is

$$P_2 = 2\int_o^{\frac{b}{4}\cot\beta} \frac{\sigma_y t^2}{4\Delta^*}(1+\sec^2\beta)\,db$$

$$= \sigma_y \frac{tb}{4}\cot\beta\left\{\sqrt{\left(\frac{2\Delta}{Kt}\right)^2+1}-\frac{2\Delta}{Kt}+\frac{1}{2\Delta/Kt}\log_n\left[\sqrt{\left(\frac{2\Delta}{Kt}\right)^2+1}+\frac{2\Delta}{Kt}\right]\right\} \qquad (11)$$

where $K \equiv 1+\sec^2\beta$.

The average stress σ for the whole plate width is therefore

$$\frac{\sigma}{\sigma_y} = [\sqrt{(\varepsilon)^2+1}-\varepsilon] + {}^1\!/\!_4\,\{-2\cot\beta[\sqrt{(\varepsilon)^2+1}-\varepsilon]$$

$$+\cot\beta\left[\sqrt{\left(\frac{2\varepsilon}{K}\right)^2+1}-\frac{2\varepsilon}{K}\right]+\frac{\cot}{2\varepsilon/K}\log_n\left[\sqrt{\left(\frac{2\varepsilon}{K}\right)^2+1}+\frac{2\varepsilon}{K}\right]\Bigg\} \qquad (12)$$

where $\varepsilon \equiv \Delta/t$.

The variation of σ/σ_y for a fixed value of ε and with different values of β is not great and the minimum value for $\varepsilon \gtrless 2$ is always given by $\beta = 45°$. Putting this value in eqn. (12),

$$\frac{\sigma}{\sigma_y} = {}^1\!/\!_2\left[\sqrt{(\varepsilon)^2+1}-\varepsilon\right] + {}^1\!/\!_4\left[\sqrt{\left(\frac{2\varepsilon}{3}\right)^2+1}-\frac{2\varepsilon}{3}\right]$$

$$+\frac{3}{8\varepsilon}\log_n\left[\sqrt{\left(\frac{2\varepsilon}{3}\right)^2+1}+\frac{2\varepsilon}{3}\right] \qquad (13)$$

As $\varepsilon \to 0$ the average stress $\sigma \to \sigma_y$. Equation (13) gives the loaddeflection curve for small ε; in the next section a correction for membrane effects is derived. However, it is found that the expression (13) dominates especially in the important region of interest, *viz.* near the plate failure load.

3.2 Membrane Action

In this analysis a very simplistic approach is followed and essentially is based on the premise that during a virtual displacement of the ends the mechanism will deform such that the surface area must increase to maintain integrity of the plate. We shall assume that all the required membrane deformation takes place at the hinge lines and at a constant stress equal to the yield stress. Thus, during a virtual change, the angle $\theta \to (\theta + d\theta)$, see Fig. 14b, and the edges of the mechanism approach each other by $^1\!/\!_2\, b\theta\, d\theta$. Also, the ridge extends by $\frac{b}{2}\cot\beta \sin\omega\, d\omega$ where β is the true angle (Fig. 14b). Using the approximation

$$\cot\beta \sin\omega \simeq \tan\theta$$

the change in perimeter ε_p of the mechanism at some height y is therefore

$$\varepsilon_p = 2b\ \theta d\ \theta\ [(1 + \tan\ \beta)y - 1] \tag{14}$$

and the plastic energy dissipated during the virtual change of state is

$$2\sigma_y\ b\ \theta d\ \theta \int_o^{\frac{b\theta}{2}} [(1 + \tan\ \beta)y - 1]\ dy = \frac{\sigma_y t}{2} b^2\ \theta^2\ d\theta \left[\frac{1 + \tan^2\beta}{1 + \tan\ \beta}\right] \tag{15}$$

The work done during the virtual change is

$$\sigma_m\ bt\ \tfrac{b}{2}\ \theta d\ \theta \tag{16}$$

where σ_m is the contribution to the average stress due to membrane action. Equating (15) and (16), we have

$$\frac{\sigma_m}{\sigma_y} = \frac{\varepsilon}{b/t}\left[\frac{1 + \tan^2\beta}{1 + \tan\ \beta}\right] \tag{17}$$

and for moderate deflections, with $\beta = 45°$

$$\frac{\sigma_m}{\sigma_y} = \frac{\varepsilon}{b/t} \tag{18}$$

The total average stress applied to the mechanism is the sum of the bending and membrane actions. Fig. 16 and 17 show the comparison of predictions of the theory developed above and experimental values obtained by SHERBOURNE and KOROL [6]. The tests were on square thin-walled tubes loaded axially and the elastic line, which was for simply-supported plates with stress-free unloaded edges [3], assumes no initial deformations. The plastic mechanism unloading line is seen to provide reasonable agreement for the maximum load and for the rate of collapse of the plates.

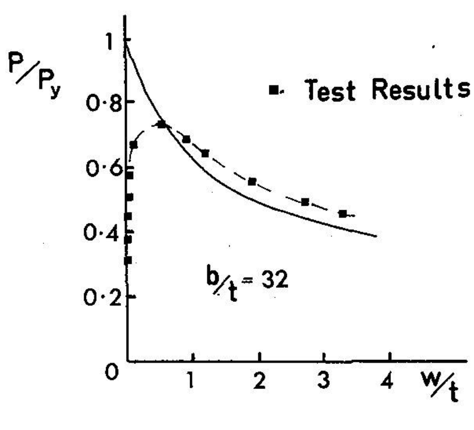

Fig. 16

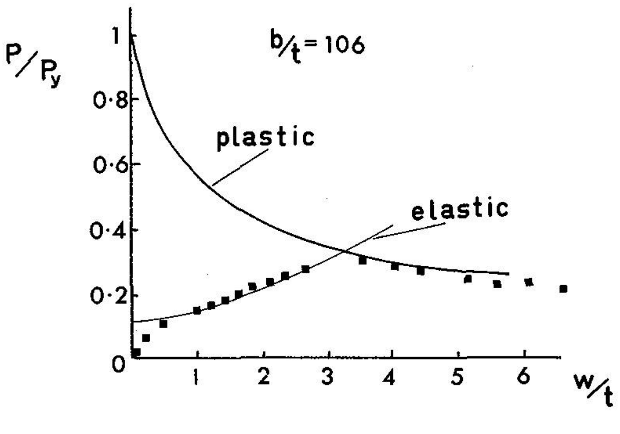

Fig. 17

4. Stiffened Plates

The results of the above plate analysis can be applied to stiffened plates loaded axially and which fail by yielding at the intersection of the plate and stiffener. Two examples are considered in detail here; they are from tests described in Reference (9) and have the geometries shown in Fig. 18 and an average yield stress of 377 MN/m^2. The longitudinal deformed shape is assumed to be as shown in Fig. 18 and the tiffener is considered to be yielding across to depth. The analysis is similar to that in Reference (9) and requires the satisfaction of the compatibility condition,

$$\alpha = \frac{\Delta^2}{\frac{b}{4}\left[\frac{t_1}{2} + h_2 - c\right]} \tag{19}$$

from which the central deflection is obtained as

$$\delta = \frac{t_1^2\, l\left(\frac{\Delta}{t_1}\right)^2}{\frac{b}{4}\left[\frac{t_1}{2} + h_2 - c\right]} \tag{20}$$

Also, equilibrium must be satisfied for the deformed position, i.e. for total axial force P,

$$P = P_{pl} + F_{sc} - F_{st} \tag{21}$$

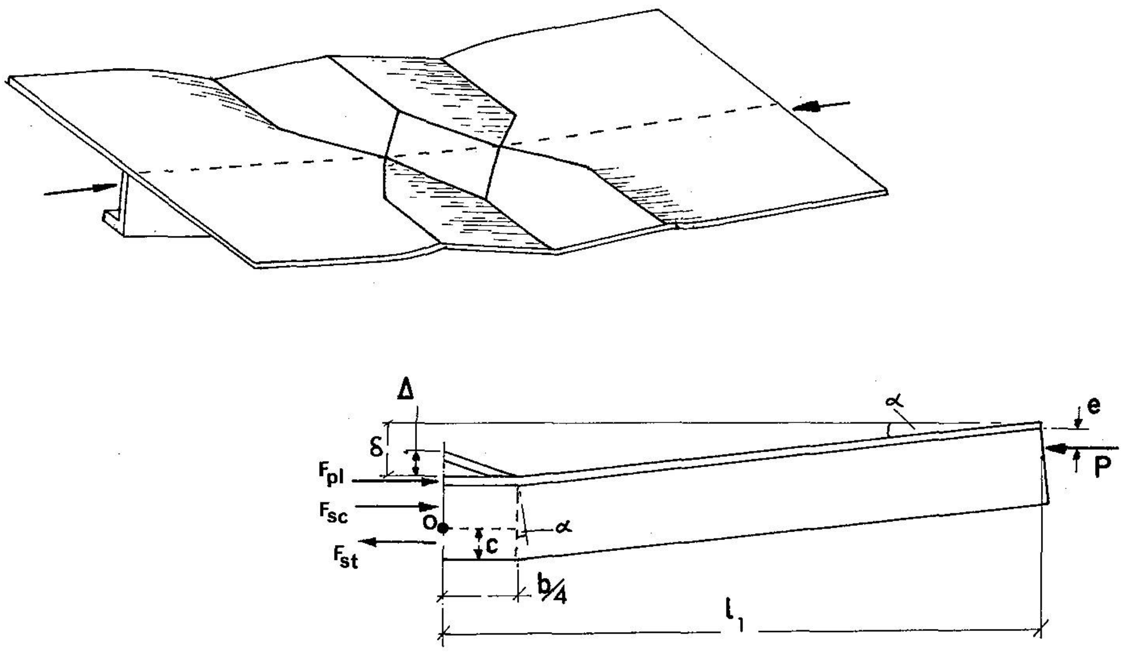

Fig. 18

and for moment equilibrium about 0,

$$F_{pl}\left[\frac{t_1}{2}+h_2-c\right]+F_{sc}\frac{h_2-c}{2}+F_{st}\frac{c}{2}=P\,(\delta+h_2-e-c) \tag{22}$$

in which the plate force F_{pl} is obtained using equations (13) and (18). For the two stiffened plate geometries tabulated in Fig. 19 the unloading line obtained by satisfying the above condition is shown in Figs. 20 and 21. Also shown there are cocorresponding theoretical results obtained by MURRAY using a mechanism indicated by Fig. 1a for plate collapse.

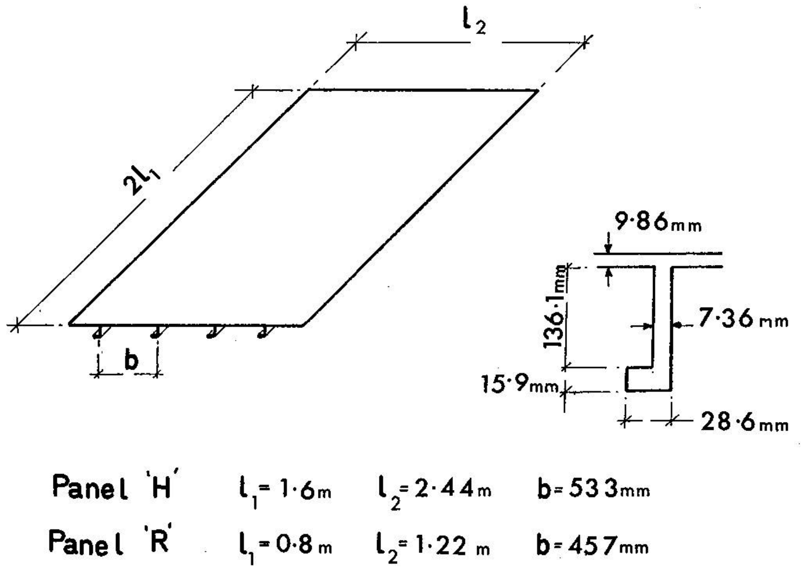

Fig. 19

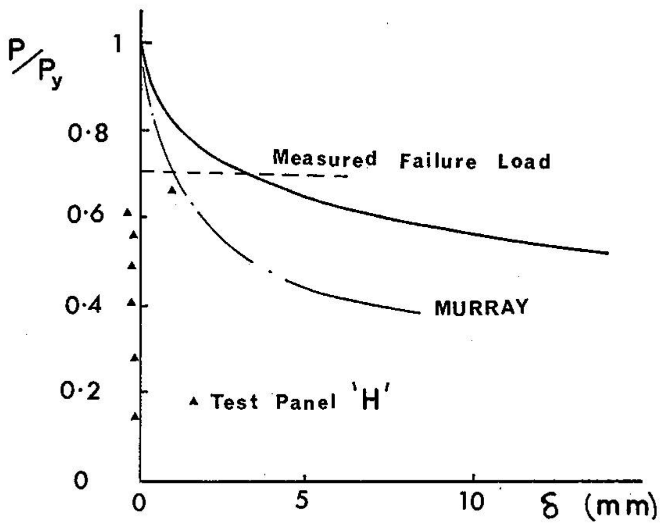

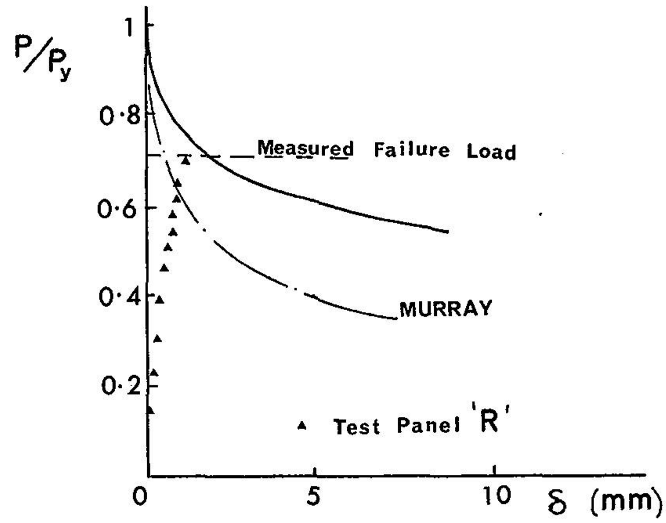

5. Discussion and Conclusions

1. Previously the behaviour of isolated struts and frameworks have been studied by superimposing two theoretical curves, one derived from elastic theory and the other from rigid-plastic theory. Adequate descriptions of strut and framework buckling phenomena have been obtained because nearly all of the energy of both the elastic and plastic modes is bending strain energy. In considering the behaviour of axially loaded plates significant amounts of energy are also stored in the form of membrane stresses. In this paper the effect of membrane (elastic) stresses on the buckling behaviour of axially loaded plates is considered. It is shown that the elastic strain energy available in this form can affect the failure load, the shape of the plastic mechanism developed during failure and the suddenness of collapse. The understanding of the failure process has been facilitated by studying the behaviour of analogous spring and link mechanisms. From these studies and laboratory observations it appears that the process of failure is as follows.

With increasing axial load eventually the plate develops a regular pattern of buckles in roughly square panels. One might expect that the plastic mechanism would also follow a similar regular pattern throughout the plate. From the studies of the spring and link analogues (Fig. 9) it is shown that the irregularity of initial imperfections plays a dominant role and instead of developing a plastic mechanism which extends right throughout the plate only one section becomes fully developed. While this is happening the buckles throughout the remainder of the plate decrease in amplitude and finally disappear after failure.

2. This analysis has been applied to published results for thin-walled square tubes and agreement between theoretical and experimental results is found to be good.

3. For the case of stiffened plates failing by plate buckling (i.e. not by stiffener buckling) (Figs. 20 and 21) the previously published analysis of Murray [9] predicts sudden collapse in contrast to laboratory observations. The mechanism used by

him is shown in Fig. 1a, and it is seen that it is equivalent to a plastic mechanism which extends throughout the plate. The only significant difference between his mechanism and the one derived here is that the outer hinge line is moved inwards (c.p. Figs. 1a and 14a). As seen in Figs. 20 and 21 this raises the plastic mechanism line, thereby allowing more gradual collapse. It is now apparent that Murray's mechanism (Fig. 1a) has the maximum separation of the outer hinges while the present mechanism (Fig. 14a) has these hinges as close together as they can be. Thus the two curves in each of Figs. 20 and 21 are bounds and the actual collapse curve (as suggested for example by Fig. 1b) will lay somewhere between them. The location of these outer hinge lines although initially near to these of Fig. 1a must approach closer to those of Fig. 14a during the failure process.

6. Acknowledgments

This work was carried out while the first author was visiting Monash University, Melbourne. He would like to record his gratitude to the Australian Road Research Board and the Lower Yarra Crossing Authority for their financial support during that period of time.

Practical hints for the Engineer and Designer

There is a continuing desire on the part of engineers to develop structural forms to give ever increasing efficiency. In many circumstances this means that structures are becoming thinner and more slender. The exact analysis of such structures, for example box girders, is extremely difficult when the non-linear effects of plasticity and buckling are included.

Nevertheless, these characteristics do in fact govern the maximum load which the structure can carry and must be included in design calculations.

As a means of circumventing the analytical problems, there is growing trend to separate the influences of buckling and plasticity. This paper is concerned with the latter and proposes a simple analysis whereby the post-buckled behaviour of stiffened plates and plate elements can be simply calculated from a plastic medianism. Also, the paper discusses, by menas of a simple model, the influence of large elastic deflections and membrane stresses on the magnitude of the collapse load.

Due to the complexity of the analysis of thin structures, it is essential that engineers and designers have a clear picture of the mechanics of the behaviour of such structures. The aim of this paper is the simple presentation of an approach to developing such a picture. With the increasing complexity of structural forms, these simple approaches will have wide application and provide an approach complementary to the more cumbersome and involved methods of computer based numerical analysis.

References

1. S.P. Timoshenko and J.M. Gere: Theory of Elastic Stability, McGraw-Hill, 1961.
2. J.M. Coan: Large Deflection Theory for Plates with Small Initial Curvature Loaded in Edge Compression. Journal of App. Mech., Vol. 18, A.S.M.E., Vol. 73, 1951.
3. A.C. Walker: The Post-Buckling Behaviour of Simply-Supported Square Plates. Aero Quart., Vol. 20, 1969.
4. R.G. Dawson and A.C. Walker: Post-Buckling of Geometrically Imperfect Plates. Journal of Struct. Div., A.S.C.E., Vol. 98, 1972.
5. T.R. Graves-Smith: A Variational Method for Large Elasto-Plastic Theory in its Application to Arbitrary Flat Plates. Proc. Int. Confer. Solid Mech., 1969.
6. A.N. Sherbourne and R.M. Korol: Ultimate Strength of Plates in Uniaxial Compression. A.S.C.E. Nat. Struct. Eng. Meeting, 1971.
7. A.N. Sherbourne, C.Y. Lian and C. Marsh: Stiffened Plates in Uniaxial Compression. Pub. I.A.B.S.E., Vol. 31, 1971.
8. N.W. Murray: The Behaviour of Thin Stiffened Steel Plates. I.A.B.S.E., Vol. 33-I, 1973.
9. N.W. Murray: Buckling of Stiffened Panels Loaded Axially and in Bending. To be published in The Structural Engineer.
10. J.A.L. Matheson: Hyperstatic Structures. Vol. 1, Chapt. 8, Butterworth 2nd Ed.
11. N.W. Murray: Das aufnehmbare Moment in einem zur Richtung der Normalkraft schräg liegenden plastischen Gelenk. Die Bautechnik, Heft 2, 1973, Seite 57.

Summary

This paper examines the behaviour of uniformly compressed rectangular thin plates when they are loaded beyond their ultimate load. The manner in which plates buckle is described, the behaviour of analogous mechanisms consisting of rigid links and springs are studied and from these studies a plate mechanism is derived. It is shown that the membrane elastic energy plays a significant role in determining the post-buckling behaviour of a thin plate.

Résumé

Dans cette contribution, on étudie le comportement de plaques minces rectangulaires sous l'influence de compressions uniformes et qui sont chargées au-dessus de leur charge ultime. On dérive le genre du voilement des plaques et on étudie le comportement de mécanismes analogues comprenant des membres rigides et des ressorts. On montre que l'énergie élastique de la membrane joue un rôle significatif dans la fixation du comportement du voilement postcritique d'une plaque mince.

Zusammenfassung

Der Beitrag untersucht das Verhalten gleichmässig gedrückter dünner rechteckiger Platten, die über ihre zulässige Last hinaus belastet werden. Die Art der Plattenbeulung wird beschrieben und das Verhalten analoger Mechanismen, bestehend aus starren Gliedern und Federn wird studiert und aus diesen Untersuchungen ein Plattenmechanismus abgeleitet. Es wird gezeigt, dass die elastische Membranenergie eine wichtige Rolle bei der Bestimmung des Nachbeulverhaltens einer dünnen Platte spielt.